

DOE/ET/53088-7

IFSR #7

NUMERICAL COMPUTATION OF RELAXATION RATES  
FOR THE  
TEST WAVE MODEL

James D. Meiss

Institute for Fusion Studies  
The University of Texas at Austin  
Austin, Texas 78712

February, 1981

NUMERICAL COMPUTATION OF RELAXATION RATES  
FOR THE  
TEST WAVE MODEL\*

James D. Meiss

Institute for Fusion Studies  
The University of Texas at Austin  
Austin, Texas 78712

February, 1981

\* Adapted from a talk presented at the "Nonlinear Properties of Internal Waves" Workshop in La Jolla, CA., January, 1981.

Weak turbulence is frequently analyzed by use of the radiative transport equation [Davidson, 1972]. This equation describes the evolution of the mean wave action spectrum under the assumption that the wave phases are random. In a homogeneous medium, with quadratic nonlinearity the waves interact in triplets satisfying the wavenumber relations

$$\underline{k} \pm \underline{l} \pm \underline{m} = 0 \quad (1)$$

The equations of motion for the amplitudes of the linear eigenmodes take the form

$$\dot{a}_{\underline{k}} + i\omega_{\underline{k}} a_{\underline{k}} = \sum_{\underline{l}, \underline{m}} \left[ \Gamma_{-} a_{\underline{l}} a_{\underline{m}} \delta_{\underline{k}-\underline{l}-\underline{m}} + \Gamma_{+} a_{\underline{l}}^* a_{\underline{m}} \delta_{\underline{k}+\underline{l}-\underline{m}} \right] \quad (2)$$

where  $\omega_{\underline{k}}$  is the mode frequency and  $\Gamma_{\pm}$  are the nonlinear coupling coefficients as functions of  $\underline{k}, \underline{l}$ , and  $\underline{m}$ .

The transport equation is obtained from (2) by use of the "random phase approximation" (RPA) [Davidson, 1972]. This approximation implies that only triads satisfying resonance conditions of the form  $\omega_{\underline{k}} \pm \omega_{\underline{l}} \pm \omega_{\underline{m}} = 0$  contribute to the transport. Schematically, the transport equation may be written

$$\frac{\partial}{\partial t} F(\underline{k}) = I(\underline{k}) - 2\nu_p(\underline{k})F(\underline{k}) \quad (3)$$

where  $F(\underline{k}) = \langle J_{\underline{k}} \rangle$  is the mean wave action density in wavenumber space, and  $I(\underline{k})$  and  $\nu_p(\underline{k})$  are functionals of the spectrum  $F(\underline{k}')$ .

Here  $I(\underline{k})$  is a positive definite quadratic functional of  $F$  which represents the flow of action into the wavenumber  $\underline{k}$ . The rate  $v_p(\underline{k})$  is linear in  $F$  and describes the effective dissipation due to the ambient wavefield\*. As indicated above, the RPA implies that both  $I$  and  $v_p$  are integrals over resonant triads.

This separation of the transport into two parts can be further elucidated by consideration of the autocorrelation function of the wave amplitude

$$b_{\underline{k}}(t) = a_{\underline{k}}(t) e^{i\omega_{\underline{k}} t} = \sqrt{J_{\underline{k}}} e^{-i(\theta_{\underline{k}} - \omega_{\underline{k}} t)} \quad (4)$$

Using a multiple time scale, averaging perturbation theory\*\* on equations (2), the autocorrelation function can be shown to obey [Pomphrey, Meiss, and Watson, 1980]:

$$\frac{\partial}{\partial t} C_{\underline{k}}(t) = (-v_p(\underline{k}) + i\delta\omega_{\underline{k}}) C_{\underline{k}}(t) \quad (5)$$

where  $v_p$  is identical to that rate in (3) and  $\delta\omega_{\underline{k}}$  is a real second order frequency shift. Therefore  $v_p$  describes the relaxation rate; as distinguished from the transport rate given by  $\frac{\partial F}{\partial t}$  in (3).

\* For non-thermal spectra it is possible to have  $v_p < 0$ .

\*\* Strictly speaking, the RPA is not used in this derivation-- the average over the fast time scale eliminates the non-resonant contribution.

In this paper we describe some numerical experiments which attempt to ascertain the validity of the RPA in determining  $v_p$ . In our "experiments" we consider a spectrum of waves which is in steady state according to (3) (an example of this is the equipartition of action equilibrium:  $F(\underline{k}) = \text{constant}$ ; however, non-equilibrium steady states could also be used). Suppose that a single wave - the test wave - is initially given a non-steady value for its action. Equation (3) then predicts exponential relaxation back to the steady state:

$$F(\underline{k}, t) = F(\underline{k}, 0) e^{-2v_p t} + \frac{I(\underline{k})}{2v_p} (1 - e^{-2v_p t}) \quad (6)$$

where  $I(\underline{k})$  and  $v_p(\underline{k})$  are constant in time since the ambient waves are in steady state. Our numerical experiments will dynamically model this process.

The model we use is the test wave (TW) Hamiltonian [Meiss, 1979]. In this system one wave - the test wave - is allowed to interact with a set of background or ambient waves. All interactions, however, that do not involve the TW are discarded.

In addition, each ambient wave is permitted to interact in only one triad.

We label the test mode by wavenumber  $\underline{k}$  and frequency  $\omega_{\underline{k}}$ , and the ambient modes with wavenumbers  $\underline{\ell}$  and  $\underline{m}$  and frequencies  $\omega_{\underline{\ell}}$  and  $\omega_{\underline{m}}$ . For triad or three wave interactions, the TW Hamiltonian is then

$$\begin{aligned}
 H = & \omega_{\underline{k}} J_{\underline{k}} + \sum_{\underline{\ell}} \omega_{\underline{\ell}} J_{\underline{\ell}} + \\
 & \sum_{\underline{\ell}, \underline{m}} \left\{ \Gamma_{-} e^{i\Theta_{-}} \delta_{\underline{k}-\underline{\ell}-\underline{m}} + \Gamma_{+} e^{i\Theta_{+}} \delta_{\underline{k}+\underline{\ell}-\underline{m}} \right\} \sqrt{J_{\underline{k}} J_{\underline{\ell}} J_{\underline{m}}} \\
 & + \text{complex conjugate} \\
 \Theta_{\pm} \equiv & \theta_{\underline{k}} \pm \theta_{\underline{\ell}} - \theta_{\underline{m}} \tag{7}
 \end{aligned}$$

Here  $J$  represents the wave action density,  $\theta$  the conjugate angle variable, and  $\Gamma_{\pm}(\underline{k}, \underline{\ell}, \underline{m})$  are the coupling coefficients as in (2). The summations are over a set of wavenumbers comprising the ambient modes.

It is easy to see that the derivation of the relaxation equation (5) [Pomphrey, Meiss, and Watson, (PMW); 1980] also applies to the TW system when the background wave spectrum is continuous. In fact, the averaging perturbation methods, in lowest order, select the "direct" interactions of the ambient waves with the test wave and discard the "indirect" interactions of the ambient waves among themselves. Higher order perturbation calculations would, of course, include increasingly more direct interactions.

The test wave model was introduced in plasma physics by Dupree [1966]. In Dupree's analysis the initial phases of the background waves were assumed random. We shall consider a similar ensemble for some of the computations below.

The TW approximation to the full dynamics is similar in character to the direct interaction approximation (DIA). In

fact the renormalization in the DIA utilizes just those interactions retained in the TW Hamiltonian [Orszag, 1977; Krommes, 1980]. Kraichnan [1963] used a TW model in a 2-d turbulence computation for comparison with the DIA. These considerations lead us to hope that the TW system will be a useful model for the description of weak turbulence.

In contrast to these expectations, numerical integration of the equations of motion leads to evidence that the TW Hamiltonian is completely integrable [Meiss, 1979]. An  $N$  degree-of-freedom Hamiltonian is integrable if there exist  $N$  independent integrals (or, roughly, constants of motion). For systems with more than one degree of freedom the required integrals often do not exist [Berry, 1978]. For the test wave system, the computations suggest integrability for an arbitrary number of triads, with arbitrary values for the parameters. The analytic form of these integrals is known [Meiss, 1980] only for the special case of resonant triads with equal coupling coefficients ( $\Gamma_{\pm} = 1$ ). Discovery of the integrals in the general case would eliminate the need for the following computations, and perhaps provide a platform from which the indirect interactions could be attacked.

Complete integrability has a dramatic qualitative effect on Hamiltonian flow. To demonstrate this we compare the trajectories of the TW system with two ambient wave pairs with those of a system in which the background waves are coupled together. The Hamiltonian for this system is

$$H = H_0 + \delta H$$

$$H_0 = \sum_{i=0}^4 \omega_i J_i + \epsilon_1 \sqrt{J_0 J_1 J_3} \sin(\theta_0 - \theta_1 - \theta_3) + \epsilon_2 \sqrt{J_0 J_2 J_4} \sin(\theta_0 - \theta_2 - \theta_4)$$

$$\delta H = \epsilon_3 \sqrt{J_1 J_2 J_3} \sin(\theta_1 - \theta_2 - \theta_3) + \epsilon_4 J_3 \sqrt{J_4} \sin(\theta_4 - 2\theta_3) \quad (8)$$

The interactions for this system are indicated in Fig. 1. Here each mode is represented by a circle and each triad by a triangle connecting the modes. The TW Hamiltonian,  $H_0$ , has only the interactions indicated by solid lines in Fig. 1; while the additional interactions, representing  $\delta H$ , are shown by dashed lines. For our computations we choose the  $\omega_i$  so that all triads are resonant.

A trajectory for the TW Hamiltonian  $H_0$ , displayed in Fig. 2a with  $\epsilon_1 = 0.67$  and  $\epsilon_2 = 0.85$ , shows that the motion is quasi-periodic with a near recurrence of the initial conditions at  $t \approx 42$ . For the trajectory of Fig. 2b the Hamiltonian is  $H = H_0 + \delta H$  where  $\epsilon_3 = 0.47$  and  $\epsilon_4 = 0.58$ . This trajectory is qualitatively more irregular, and if it is periodic must have a much longer period. A more definitive indication of this irregularity or "stochasticity" is obtained by considering the rate of separation of neighboring trajectories [Berry, 1978]. In Figures 2c and 2d the phase space "distance" between orbits [Meiss, 1979] that had an initial separation of  $10^{-6}$  is plotted. For the TW system this distance increases only linearly with time as is characteristic of an integrable system. The second



system exhibits exponential growth of the separation which saturates when it becomes of order the "diameter" of the energy surface. This strong instability makes accurate numerical integration of the equations virtually impossible; in fact if the equations are integrated backwards beginning with the state at  $t = 60$ , the time reversed orbit follows the original for only 25 time units.

Relaxation rates for nonlinear wave interactions are obtained by calculation of correlation functions. The auto-correlation of the TW amplitude is defined by

$$C_{\tilde{k}}(\tau) \equiv \frac{\langle \tilde{b}_{\tilde{k}}^*(t) \tilde{b}_{\tilde{k}}(t + \tau) \rangle_t}{\langle \tilde{J}_{\tilde{k}}(t) \rangle_t} \quad (9)$$

where  $\langle \rangle_t$  denotes time average. Figures 2e and 2f show  $C_0$  for the two Hamiltonians of eq. (8). The relaxation rates,  $\nu$ , computed from the figures, could be compared with the  $\nu_p$  of (5). Similar computations for 2-d turbulence have been done by Kells and Orszag [1978].

The rate computed in this manner for the TW system is not very useful because its trajectories are not ergodic. This implies that  $\nu$  depends upon the orbit along which the time average is taken - that is,  $\nu$  depends in detail upon the wave phases as well as amplitudes. We can circumvent this problem for the TW system by using an ensemble average in place of the time average. This is a reasonable procedure since in an

experiment, most of the integrals of the TW system would probably not be measured or controlled. All that is typically known is the mean wave action. We, therefore, choose an ensemble that depends only on these actions and for simplicity use the Gaussian distribution with random phases. In our computations the initial TW action-amplitude is held fixed while the initial conditions of the ambient modes are picked randomly from the ensemble. The correlation function is now defined by

$$C_{\tilde{k}}(\tau) = \frac{\langle b_{\tilde{k}}^*(0) b_{\tilde{k}}(\tau) \rangle}{J_{\tilde{k}}(0)} \quad (10)$$

We begin with an example for which  $J_{\tilde{k}}(0)$  is much smaller than  $\langle J_{\tilde{k}} \rangle$ . Using  $N = 100$  initial conditions we find that  $\langle J_{\tilde{k}}(t) \rangle$  converges and exhibits the form shown in Fig. 3. The salient features of this figure are a rapid rise of the TW action by a factor of 100 in the first 20 time units, followed by small oscillations about some stationary value. Qualitatively, this is precisely what one would expect from the transport theory (e.g. equation (6)). In contrast to this, the computed  $C_{\tilde{k}}(t)$  does not converge with  $N = 100$ . In fact since the mean action (which is also the variance of the random variable  $b_{\tilde{k}}(t)$ ) increases by a factor of 100, the error in the computation of  $C_{\tilde{k}}(t)$  also becomes large. Proper computation of the correlation function in this case would require more than  $10^4$  initial conditions.

The "steady state" value for the TW action,  $\langle J_{\tilde{k}}(\infty) \rangle$  appears to depend upon its initial value. The curve for  $\langle J_{\tilde{k}}(\infty) \rangle$  as presented in Fig. 4 is closely fit by the function

$$\langle J_{\tilde{k}}(\infty) \rangle = 4.0 \langle J_{\tilde{k}} \rangle_{\text{eq}} + \frac{1}{3} J_{\tilde{k}}(0) \quad (11)$$

where  $\langle J_{\tilde{k}} \rangle_{\text{eq}}$  is the equilibrium level expected from the initial ensemble (for example equipartition of action). In the computations of Fig.4 only 15 triads were retained, and it is probable that the dependence of  $\langle J_{\tilde{k}}(\infty) \rangle$  on  $J_{\tilde{k}}(0)$  is due to the size of the TW action relative to the total ambient field action. As the number of triads becomes large this effect should disappear.

The dependence of  $\langle J_{\tilde{k}}(\infty) \rangle$  on other parameters of the Hamiltonian (1) can be determined by scaling. If the ambient actions are increased by a factor  $\lambda$  ( $\langle J_{\tilde{l}} \rangle_{\text{eq}} \rightarrow \lambda \langle J_{\tilde{l}} \rangle_{\text{eq}}$ ), then the value of  $\langle J_{\tilde{k}}(\infty) \rangle$  is also increased by  $\lambda$ . However if the coupling coefficients are scaled by  $\lambda$  ( $\Gamma \rightarrow \lambda \Gamma$ ) then  $\langle J_{\tilde{k}}(\infty) \rangle$  is unchanged.

The computation of relaxation rates necessitates consideration of resonance phenomena. As is well known, the Langevin and transport rates are given by integrals over resonant triads. For finite amplitude nonlinearities we still expect that the most important triads will be resonant; however, non-resonant triads will also contribute. Define the resonance mismatch by

$$\Delta\omega_{\pm} \equiv \omega_{\tilde{k}} \pm \omega_{\tilde{l}} - \omega_{\tilde{m}} \quad (12)$$

For any two-dimensional system, the resonance condition ( $\Delta\omega = 0$ ) defines a curve in wavenumber space (see e.g. Fig. 5). We will determine the effect of non-resonant triads by including triads in some band  $|\Delta\omega| \leq \Delta_{mx}$  about resonance. Triads are picked on a rectangular grid in wavenumber space with spacing  $\Delta k$ . Our procedure is to compute an action relaxation rate for increasing values of  $\Delta_{mx}$  until further increases have no effect on the value of the rate. In the computations of [MPW, 1979] we assumed that the relaxation is exponential and computed

$$v_{\text{exp}} = \frac{\Delta \log \langle J_{\tilde{k}} \rangle}{\Delta t} \quad (13)$$

averaged over the time it takes  $\langle J_{\tilde{k}} \rangle$  to double. Values of  $v_{\text{exp}}$  for various  $\Delta k$  are shown in Fig. 6. It is seen that  $v_{\text{exp}}$  increases as more non-resonant triads are included until  $\Delta_{mx} \approx 0.1$ .

In general we expect that the required value of  $\Delta_{mx}$  will scale with the nonlinear timescale. Therefore a converged value for  $v$  will be obtained if  $\Delta_{mx}$  is chosen, self-consistently to be a few times  $v$ . This is in agreement with our expectations from resonance broadening theory.

The values of  $v_{\text{exp}}$  in Fig. 6 appear to be relatively independent of the grid spacing  $\Delta k$ . This implies that the number of triads included has little effect on the relaxation rate. While this is serendipitous for our computations, it is also unexpected because the Langevin and transport theories

are valid only when the spectrum is continuous. Practically this implies that the time scale associated with the grid spacing should be long compared to the nonlinear time scale, or

$$\Delta k/v_{gr} \ll \nu \quad (14)$$

where  $v_{gr}$  is the group velocity. This condition is not satisfied by our computations. In fact there are cases displayed in Figure 6 for which the inequality (14) is reversed!

The exponential rate obtained from (13) is not appropriate for comparison with the transport theory result (6). In fact (6) gives a relaxation that is nearly linear in time:

$$\frac{\Delta \langle J_{\tilde{k}}(t) \rangle}{\Delta t} \approx 2\nu_p \left( \langle J_{\tilde{k}}(\infty) \rangle - \langle J_{\tilde{k}}(t) \rangle \right) \quad (15)$$

providing  $\nu_p \Delta t \ll 1$ . This rate is therefore linear providing  $\langle J_{\tilde{k}}(t) \rangle$  is small compared to the steady state value.

To test (15) we present, in Figure 7, a log-log plot of the action versus time. This figure shows that  $\langle J_{\tilde{k}}(t) \rangle$  grows as  $t^2$  until it reaches the steady state value at  $t = t_s$ . In addition, the growth rate in Figure 7 increases with  $\Delta_{mx}$  so long as  $\Delta_{mx} t_s \lesssim \pi$ .

This behavior can be explained by considering the equations of motion (2) for the amplitudes  $b$  defined in (4):

$$b_{\tilde{k}} = \sum_{\text{triads}} \Gamma_{\pm} b_{\tilde{\ell}} b_{\tilde{m}} \delta_{\tilde{k} \pm \tilde{\ell} - \tilde{m}} e^{i\Delta\omega_{\pm} t} \quad (16)$$

Assuming that the background wave amplitudes are approximately constant since  $b_{\tilde{k}}$  is small, the average action is roughly

$$\langle J_{\tilde{k}}(t) \rangle \sim \sum_{\text{triads}} |\Gamma_{\pm}|^2 \langle J_{\tilde{\ell}} \rangle \langle J_{\tilde{m}} \rangle \delta_{\tilde{k} \pm \tilde{\ell} - \tilde{m}} \left| \int_0^t e^{i\Delta\omega_{\pm}\tau} d\tau \right|^2 \quad (17)$$

The sum over triads can be approximately transformed into integrals along and across resonance curves, yielding

$$\langle J_{\tilde{k}}(t) \rangle \sim A \int_{-\Delta_{\text{mx}}}^{\Delta_{\text{mx}}} d\omega \left| \int_0^t e^{i\omega\tau} d\tau \right|^2 \quad (18)$$

It is easy to see that (18) implies

$$\langle J_{\tilde{k}}(t) \rangle \sim \begin{cases} 8\Delta_{\text{mx}} t^2 A & \Delta_{\text{mx}} t \ll \pi \\ 4\pi t A & \Delta_{\text{mx}} t \gg \pi \end{cases} \quad (19)$$

In Fig. 7,  $\Delta_{\text{mx}} t \lesssim \pi$  so that the quadratic law applies. Equation (19) also explains the dependence of the growth rate of Fig. 7 on  $\Delta_{\text{mx}}$ .

The linear growth for larger  $\Delta_{\text{mx}}$  is displayed in Fig. 8 (taken from Fig. 4 of MPW, 1979). The break in slope from  $t^2$  to approximately  $t$  occurs at  $\Delta_{\text{mx}} t = \pi$  as given by (19). It is clear from Fig. 8 and from (19) that the action at some time  $t \gtrsim \pi/\Delta_{\text{mx}}$  is independent of the value of  $\Delta_{\text{mx}}$ . Therefore if one is interested,

for example, in the saturation time, it is sufficient to choose  $\Delta_{mx} = \pi/t_s$  to obtain a converged result for  $t_s$ .

In conclusion, the dynamical computations qualitatively verify weak turbulence theory. In addition, quantitative comparison of the dynamical rate with  $v_p$  should be possible providing the time integration is carried beyond the point  $\Delta_{mx} t = \pi$ . Surprisingly, the computed relaxation rates are insensitive to the number of triads in the system.

#### Acknowledgements

The author is indebted to W. Horton and M. N. Rosenbluth for discussing and reading the manuscript. Much of the work reported in this paper was done in collaboration with K. M. Watson and N. Pomphrey. This project was partially supported by the ONR under contract N00014-78-C-0050 and DOE Contract DE FG05-80ET-53088.

References

1. Berry, M. V., 1978, "Regular and Irregular Motion", in Topics in Nonlinear Dynamics, S. Jorna (ed.), AIP, New York.
2. Davidson, R. C., 1972, Methods in Nonlinear Plasma Theory, Academic, New York.
3. Dupree, T. H., 1966, "A Perturbation Theory for Strong Plasma Turbulence", Phys. Fluids 9, 1773.
4. Kells, L. C. and Orszag, S. A., 1978, "Randomness of Low-Order Models of Two-Dimensional Inviscid Dynamics", Phys. Fluids 21, 162.
5. Kraichnan, R. H., 1963, "Direct Interaction Approximation for a System of Several Interacting Shear Waves", Phys. Fluids 6, 1603.
6. Krommes, J. A., 1980, "Renormalization and Plasma Physics", Princeton Plasma Physics Laboratory, PPPL-1568.
7. Meiss, J. D., 1979, "Integrability of Multiple Three-Wave Interactions", Phys. Rev. A19, 1780.
8. Meiss, J. D., Pomphrey, N., and Watson, K. M., 1979, "Numerical Analysis of Weakly Nonlinear Wave Turbulence", Proc. Natl. Acad. Sci. USA 76, 2109.
9. Meiss, J. D., 1980, "Statistical Dynamics of Weakly Non-linear Internal Waves" Ph.D. Thesis, University of California at Berkeley, unpublished.
10. Orszag, S.A., 1977, "Lectures on the Statistical Theory of Turbulence", in Fluid Dynamics, Ballien and Peube (eds.), Gordon and Breach.
11. Pomphrey, N., Meiss, J. D., and Watson, K. M., 1980, "Description of Nonlinear Internal Wave Interactions Using Langevin Methods", J. Geophys. Res. 85, 1085.



Figure Captions

1. The interactions of the Hamiltonian of equation (8).
2. Trajectories for the Hamiltonian  $H_0$  (a) and  $H_0 + \delta H$  (b) from equation (8). Separation of nearby orbits for  $H_0$  (c) and  $H_0 + \delta H$  (d). TW correlation function for  $H_0$  (e) and  $H_0 + \delta H$  (f).
3. Relaxation of TW action for an ensemble average over ambient initial conditions. Taken from MPW [1979].
4. Dependence of "steady state" action on initial action with 15 ambient triads.
5. Example of a resonance curve for a two-dimensional system. For details see Meiss [1980].
6. Computed values of the relaxation rate  $\nu_{\text{exp}}$  by equation (9) for various  $\Delta k$  and  $\Delta_{\text{mx}}$ .
7. Plot of TW action versus time on log-log scale showing quadratic growth.
8. TW action showing contribution of non-resonant triads.

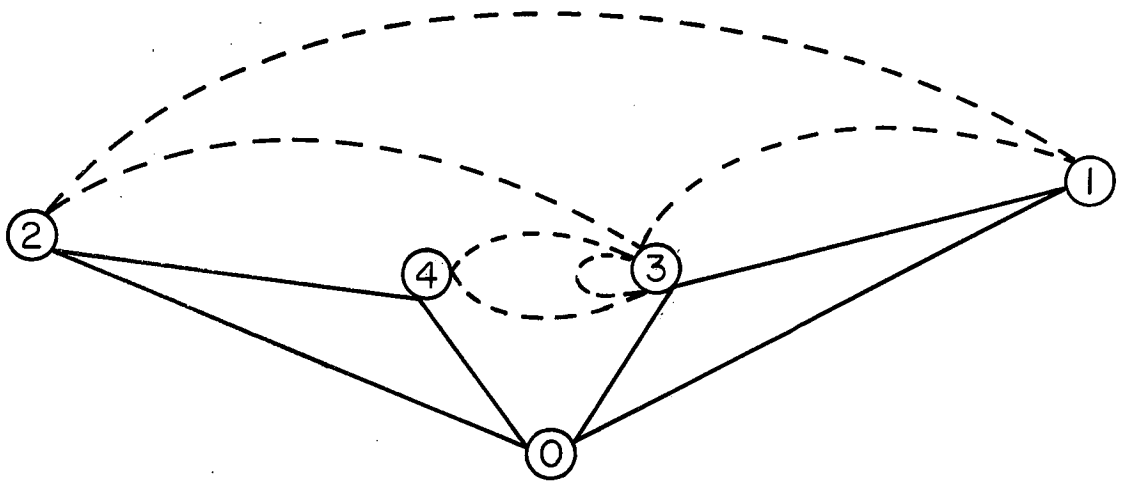


FIG. 1

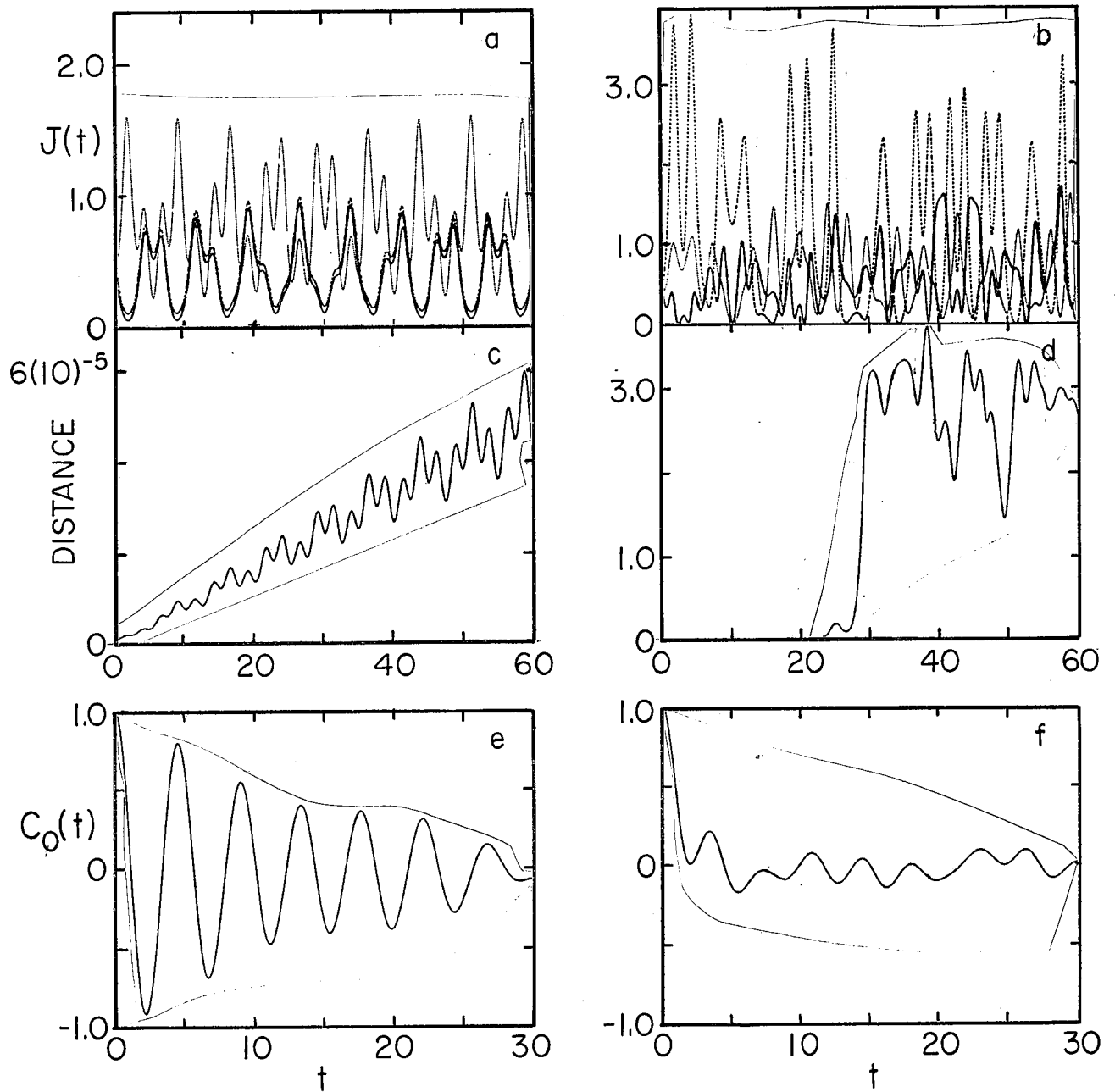


FIG. 2

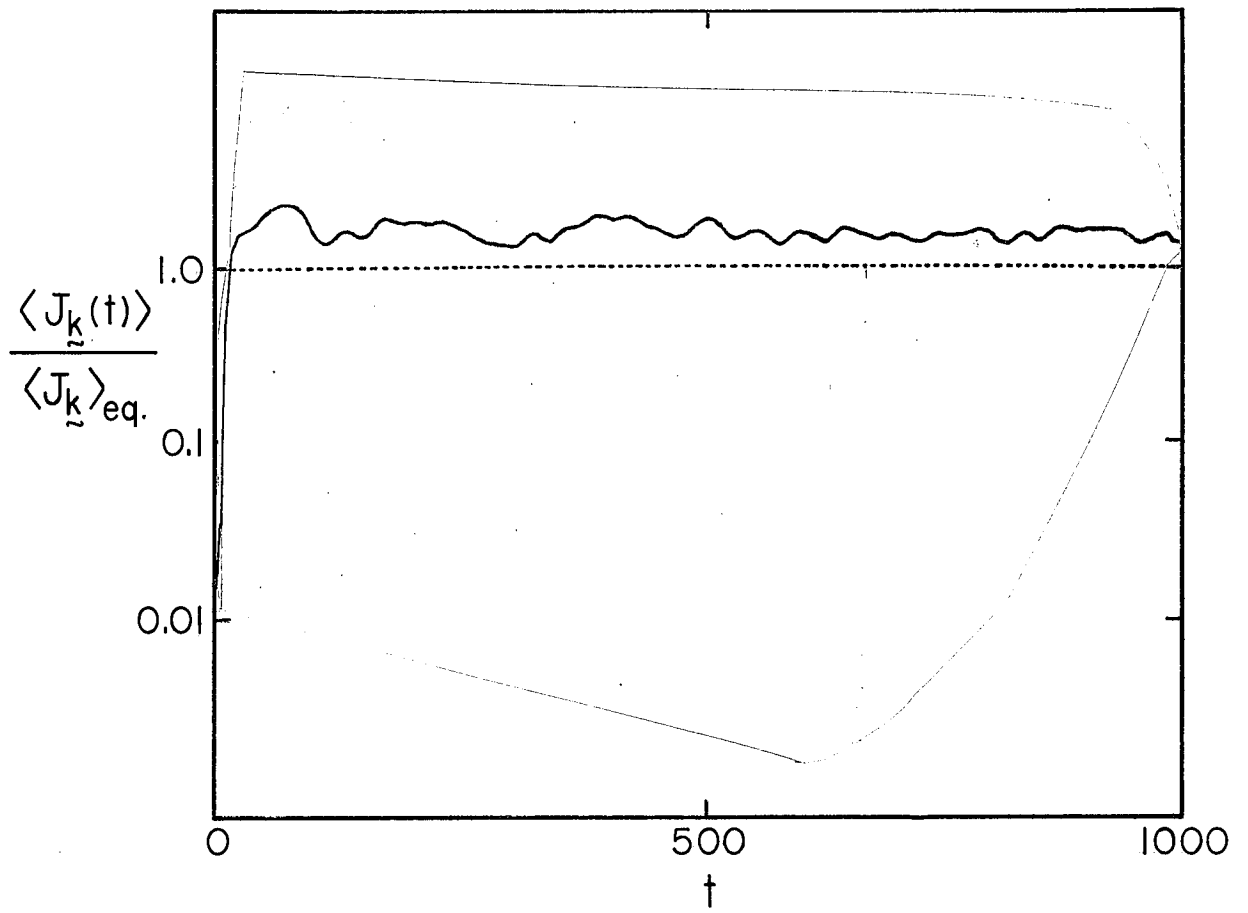


FIG. 3

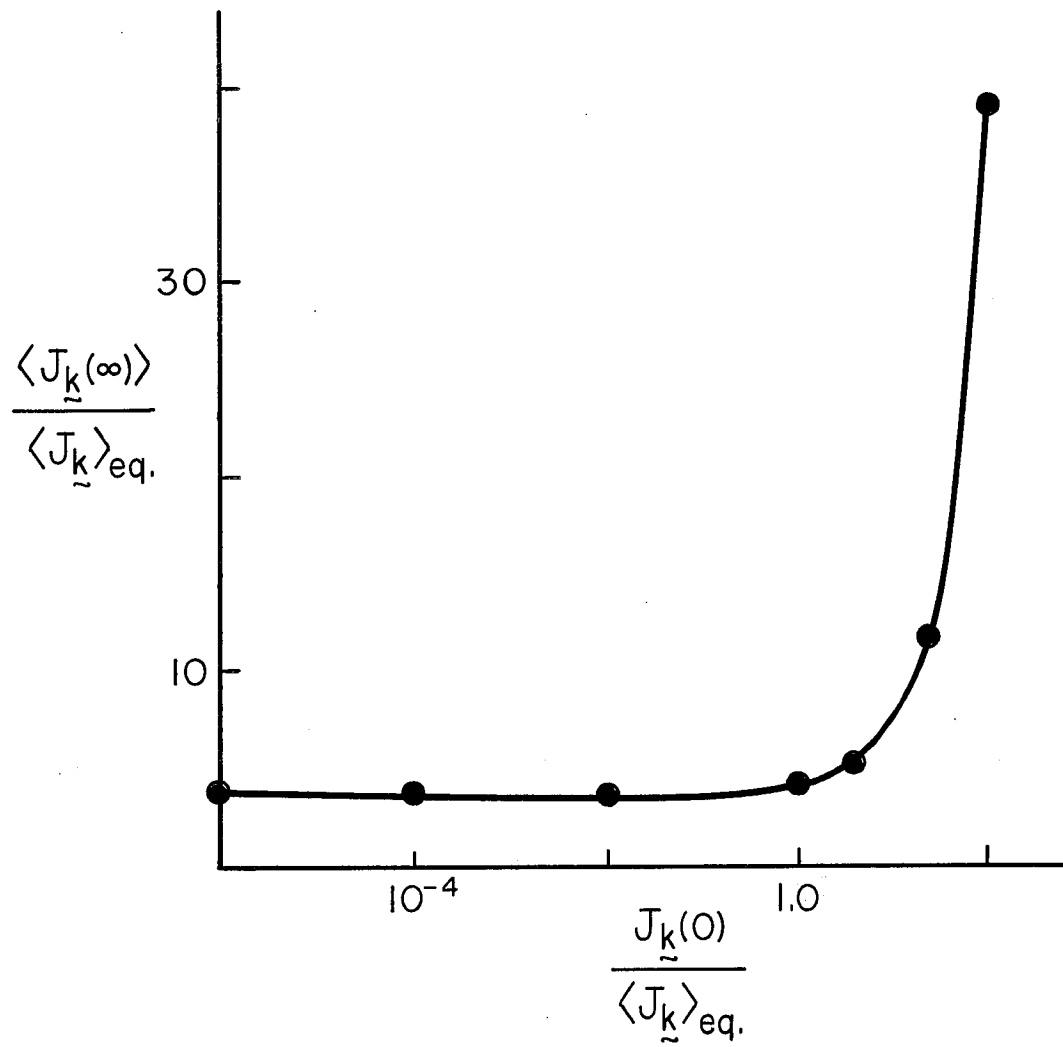


FIG. 4

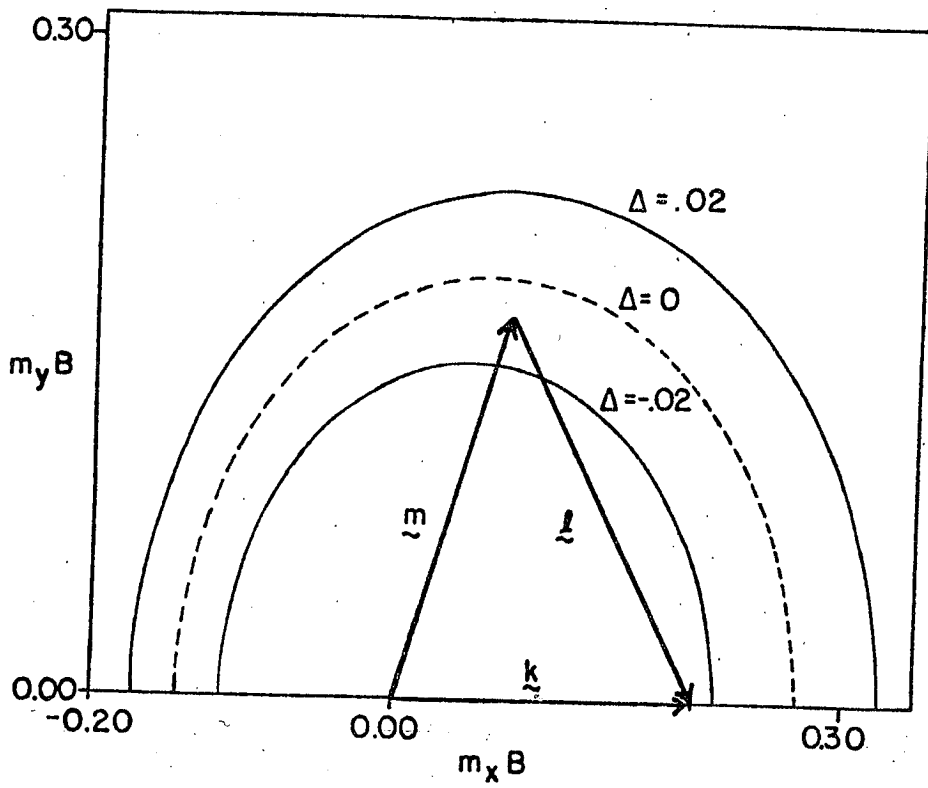


FIG. 5

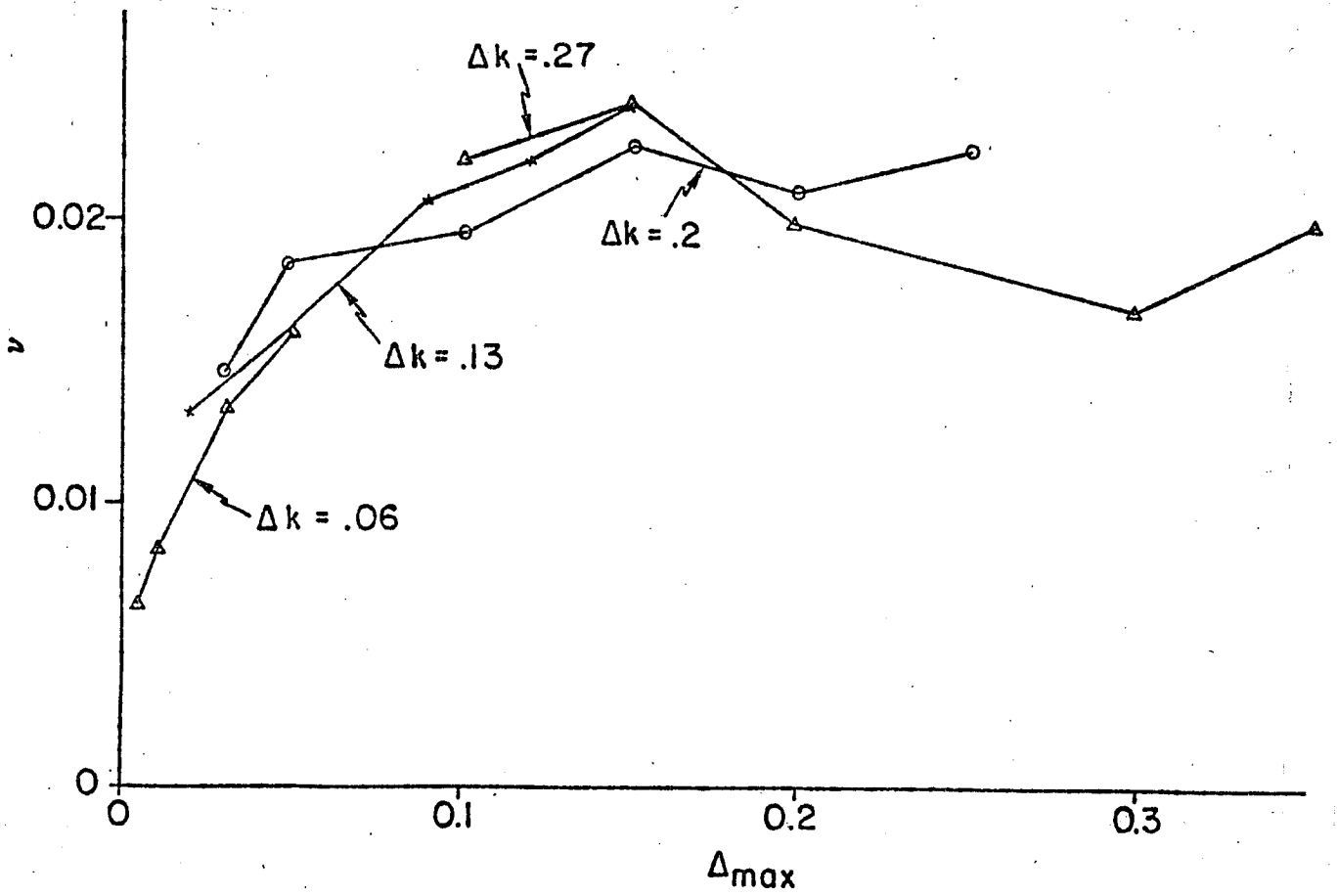


FIG. 6

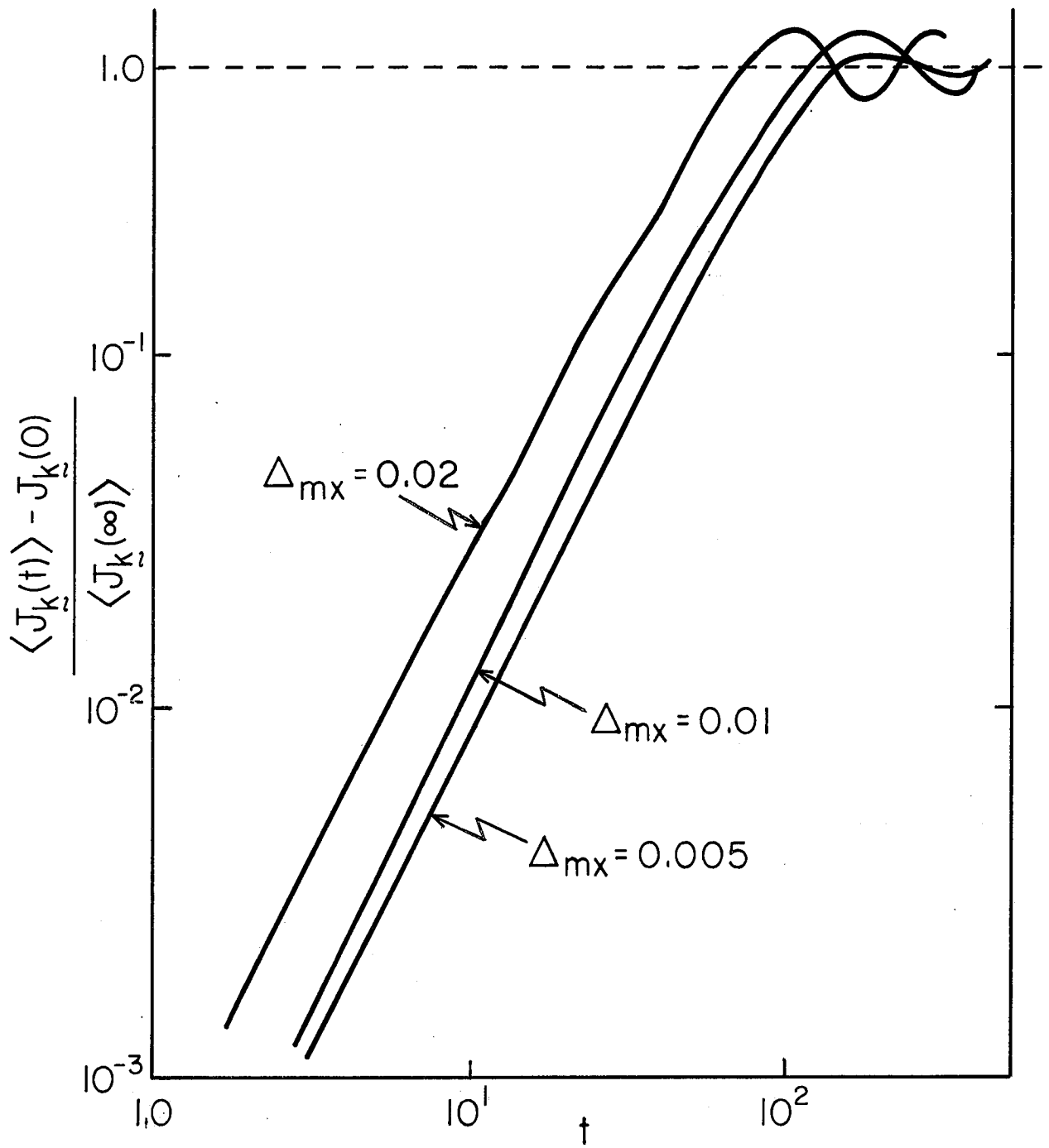


FIG. 7



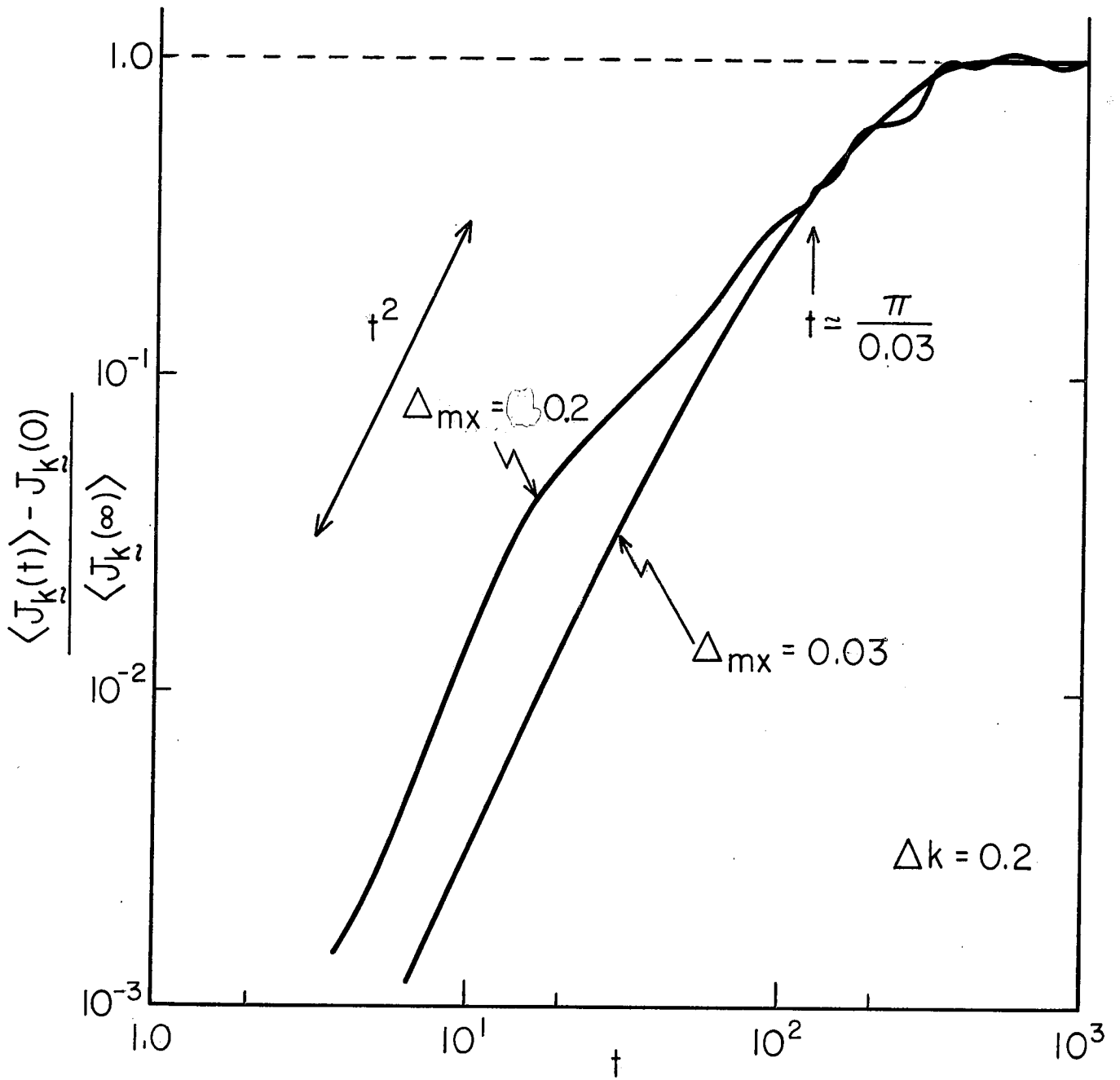


FIG. 8